Nanoscale

COMMUNICATION

View Article Online
View Journal | View Issue

Cite this: *Nanoscale*, 2014, **6**, 9536

Graphene nanoarchitecture in batteries†

Di Wei,* Michael R. Astley, Nadine Harris, Richard White, Tapani Ryhänen and Jani Kivioja

Received 17th April 2014
Accepted 18th June 2014

DOI: 10.1039/c4nr02089h

www.rsc.org/nanoscale

We compare three different carbon nanoarchitectures used to produce standard coin cell batteries: graphene monolayer, graphite paper and graphene foam. The batteries' electrochemical performances are characterised using cyclic voltammetry, constant-current discharge and dynamic galvanostatic techniques. Even though graphene is the fundamental building block of graphite its properties are intrinsically different when used in batteries because there is no ion intercalation in graphene. The nanoarchitecture of the graphene electrode is shown to have a strong influence over the battery's electrochemical performance. This provides a versatile way to design various battery electrodes on different demands.

Traditionally bulk graphite is used in lithium metal batteries (LBs) and lithium ion batteries (LIBs) because it affords high energy density. One of the reasons graphite has become the industry standard material is because of its effective Li^+ ion intercalation properties,[1,2] where Li^+ ions are inserted between the graphene layers. However, this has the drawback of causing slow, diffusion limited, recharging times because a reverse voltage is needed to remove the Li^+ ions from the graphite and force them back from the cathode to the anode *via* the electrolyte.

An increasing amount of research has focussed on improving the energy density and power density of LBs/LIBs by replacing the graphite with different carbon materials, such as carbon nanotubes, fullerenes and graphene-based materials.[3,4] These 'graphenes' are mostly either multi-layer graphenes or reduced graphene oxides containing defects and contaminants, and not possessing some of the intrinsic physical properties of pristine graphene that can be made with the chemical vapour deposition (CVD) method. Recently we have shown that CVD-grown monolayer graphene can work as a LB electrode.[5] Even though graphene is the building block of graphite[6], perfect monolayer graphene has many unique properties that graphite does not possess, like quantum capacitance. Also, it has been reported that charge flows at higher speeds in such two-dimensional (2D) nanoflakes than in bulk compounds.[7,8] Graphene conducts electricity even better than theory predicts on steps etched in silicon carbide.[8]

Reports describe repulsive Coulombic forces between Li^+ at the graphene electrode[9] as well as an inability for Li^+ to intercalate or absorb strongly to the surface of defect-free graphene.[10] Jang *et al.*[11] recently developed a combined high power (100 kW per kg per cell) and high energy density device (160 Wh per kg per cell) based on porous electrodes with large amounts of graphene surfaces in direct contact with the electrolyte. The use of graphene, as opposed to graphite, allowed the Li^+ to reach the interior graphene surfaces without the need to undergo intercalation. After recharging, *via* an external source, enormous fluxes of Li^+ ions were quickly released from the cathode to the anode and re-established the initial electrochemical potential.

Despite numerous publications about different carbon materials and structures including the ultrathin graphite foam structures,[12] there have been few attempts to directly compare different graphene nanoarchitectures in a systematic manner. In this manuscript we have examined three different carbon nano-architectures: monolayer graphene, graphite paper (stacked multi-layered graphene) and graphene foam (monolayer graphene grown on a microporous Cu foam substrate).

The monolayer graphene sample was commercially bought from Graphenea Ltd., and detailed results from this sample have been reported previously.[5] Briefly, the monolayer graphene film was grown by chemical vapour deposition (CVD) on top of a copper foil substrate in an Aixtron CVD reactor. After growth, characterisation by Raman spectroscopy, transmission electron microscopy and selected area electron diffraction confirmed the defect-free monolayer nature of the graphene.

Graphene coated on Cu foam was purchased from Graphene supermarket. A copper foam template is used as the substrate to grow graphene by a similar CVD process to the monolayer

Nokia R&D UK Ltd, Broers Building, 21 J. J. Thomson Avenue, CB3 0FA, Cambridge, UK. E-mail: di.wei@nokia.com

† Electronic supplementary information (ESI) available: Morphologies of graphene battery electrodes after discharge, energy capacities of batteries and several hundred times battery discharge results. See DOI: 10.1039/c4nr02089h

graphene sample. Graphene on Cu foam can be considered as a three-dimensional scaled-up version of monolayer graphene on Cu foil.

Graphite paper was purchased from SIGRAFLEX® of SGL Group; it was manufactured from expanded natural graphite, a homogeneous material without adhesives or binders. This prevents any electrochemical influence from chemical additives affecting the results.

The different carbon materials were used to construct standard 2032 coin-cell batteries [Fig. 1(a)]. The monolayer graphene on Cu-foil/graphene on Cu foam/graphite paper was used directly as the working electrode (cathode) with the Li-foil as the counter electrode (anode). The polymer electrolyte acts as a separator between the anode and cathode and is composed of a poly(ethylene glycol) borate ester, which enhances Li^+ transport and makes it comparable with conventional liquid organic electrolytes at room temperature.[13] Additionally the polymer electrolyte was wetted by 1 M solution of $LiPF_6$ in a 1 : 1 (v/v) mixture of ethylene carbonate and diethyl carbonate. The coin-cells were assembled within an MBraun glovebox (H_2O < 0.1 ppm, O_2 < 0.1 ppm) filled with inert Ar gas.

The advantages of using the coin-cell structure are twofold: firstly the direct electrochemistry of graphene may be studied without the need to transfer the graphene from Cu to other substrates; and secondly the electrochemical influence of Cu is negated due to the graphene layer. It should be noted that our graphene batteries are classed as Li-metal batteries as opposed to a conventional LIB, where the anode is comprised of graphite.

The electrochemical properties of the assembled coin-cell were studied with a Maccor battery tester and Autolab while cyclic voltammogram measurements were taken with Autolab. The following results have been repeated on multiple battery samples, with similar behaviour observed throughout. Additionally, parallel experiments using pure Cu foil (without graphene or graphite) showed no open circuit voltage, confirming that the graphene/graphite is responsible for these results.

Cyclic voltammetry (CV) measurements were used to examine the Li^+ interactions with the graphene surface. Three CV cycles between 0 V and 3 V (measured *versus* the Li anode) at a scan rate of 0.1 mV s^{-1} are shown in Fig. 2.

Due to the formation of the solid electrolyte interface (SEI) layer, the current density of the first cycle is largest when compared with the second and third cycles, which is also apparent when monolayer graphene is chemically modified.[14] The cathodic peak at ~1.0 V in Fig. 2(a) has been observed previously in monolayer graphene on Cu in polymer electrolyte.[9]

In conventional LIBs the intercalation of Li^+ into graphite causes the appearance of well-defined peaks from 0 V to ~0.5 V.[5,9] There are no obvious peaks below 0.5 V for the three CV cycles shown in Fig. 2(a) confirming that there is no intercalation of Li^+ in the monolayer graphene.[11] By way of contrast, Fig. 2(b) shows very sharp Li^+ insertion and extraction peaks at ~0 V and ~0.5 V respectively, showing that intercalation occurs in the graphite paper. The graphene on Cu foam sample (Fig. 2(c)) does not show peaks from Li^+ intercalation near 0 V, indicating that the coating on the Cu foam is indeed mono/few layer.

Intercalation of Li^+ ions has a detrimental effect on the structural integrity of the electrode. We observed this directly by the level of degradation suffered by the graphite paper battery

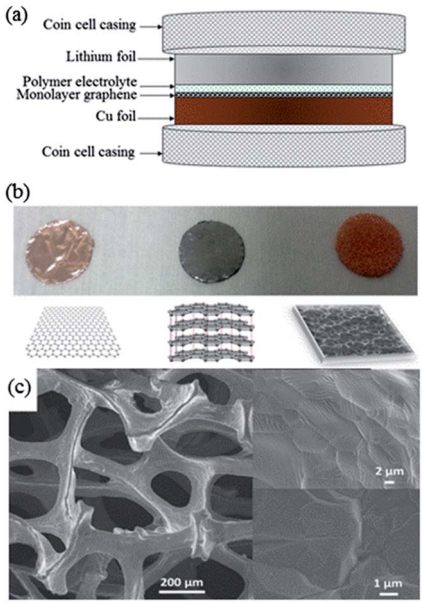

Fig. 1 (a) Cross-sectional view of fabricated coin-cell device with monolayer graphene battery electrode; (b) electrodes made from monolayer graphene on Cu foil (left), graphite paper (centre) and CVD graphene on Cu foam (right); (c) scanning electron micrograph of CVD graphene on Cu foam.

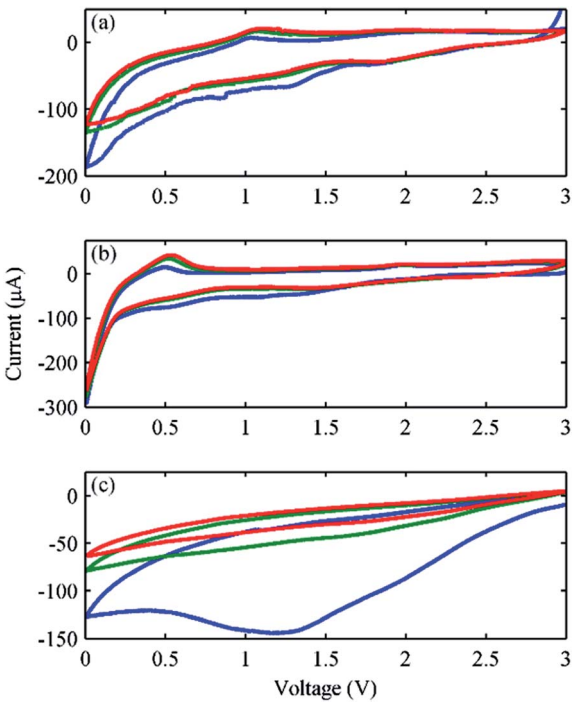

Fig. 2 CV measurements between 0 V and 3 V (measured *versus* the anode). First (blue), second (green) and third (red) cycles are shown for batteries made using (a) monolayer graphene, (b) graphite paper and (c) graphene foam.

during long-term discharge tests (ESI Fig. S1†). The monolayer graphene and graphene foam batteries showed no such degradation, consistent with the CV observations that no Li^+ intercalation takes place in graphene.

Discharge curves for the batteries are presented in Fig. 3. The batteries were discharged with a 0.5 mA load current until 0 V output voltage was reached. Open circuit potentials of ~2.25 V for the three cells are similar to other carbon based materials such as carbon nanotubes and pristine graphene *etc.*[3,4] In Fig. 3, a plateau below 1.2 V that correlates with the formation of an SEI film was observed in all three batteries.[15] The continuous voltage drop observed from 0.8 V until the end of discharge at 0.01 V has been ascribed to the 'space charge' region.[16] For the size of standard 2032 coin cell (2 cm diameter), the energy capacity at first discharge cycle for the monolayer graphene is about 0.009 mA h, for graphite paper is about 0.06 mA h and for graphene foam is about 1.55 mA h.

After the first discharge shown in Fig. 3 the discharge current was reduced to 0 A for 5 minutes, then the battery was recharged with a 0.5 mA current until 3 V. Voltages recovered gradually after the discharge and once the charging current of 0.5 mA was applied the voltage immediately reaches 3 V. As ESI Fig. 2† shows, the energy capacities drop in the forthcoming cycles for all three cells. After 10 times discharge charge cycles at a current of 0.5 mA, the energy capacity for battery made from monolayer graphene drops to 0.001 mA h, graphite paper to 0.005 mA h and graphene foam to 0.012 mA h.

The dynamic properties of the batteries were further studied using galvanostatic measurements. The batteries were repeatedly discharged under a constant current (I_{load}) for 2 seconds and then allowed to recover for 30 seconds at 0 A. In Fig. 4 the results of four discharge/recovery cycles are presented, taken with load currents of 100 μA, 250 μA and 500 μA. In all cases a substantial recovery of the battery voltage occurs during the recovery period. It should be noticed that the gravimetric current value (A g^{-1}) applied on graphene electrode is actually much higher than that applied on graphite considering the huge mass difference (ESI†). However, we can still see stable energy capacities for graphene based electrodes, which indicates graphene based electrodes have much higher discharge-rate.

The discharge/recovery cycle features a clear double-exponential decay. A heuristic equivalent circuit model was developed to describe this behaviour featuring two RC elements (inset of Fig. 4); we note that this model shows strong similarities with the double-polarisation model developed by He *et al.* to describe LIBs.[17] The battery output voltage (V_{out}) is defined by the coupled equations:

$$V_{out} = V_o - V_1 - V_2$$

$$C_1 \frac{dV_1}{dt} = I_{load} - \frac{V_1}{R_1}$$

$$C_2 \frac{dV_2}{dt} = I_{load} - \frac{V_2}{R_2}$$

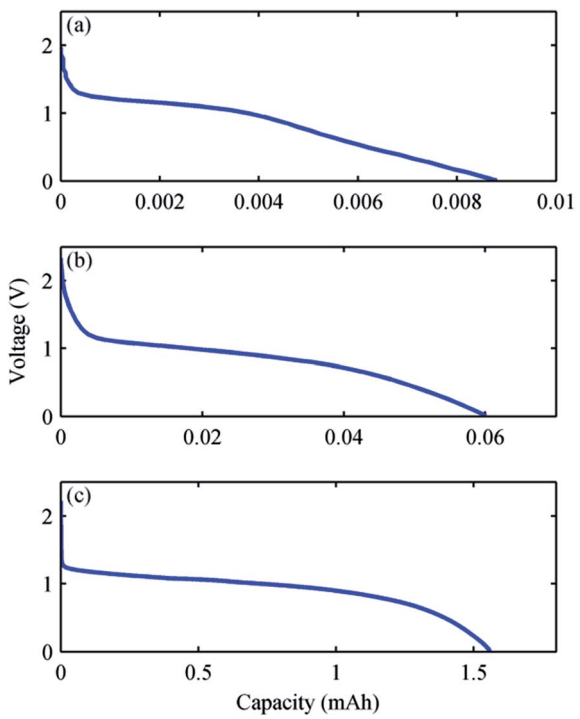

Fig. 3 First discharge curve under current of 0.5 mA for batteries made using (a) monolayer graphene, (b) graphite paper and (c) graphene foam.

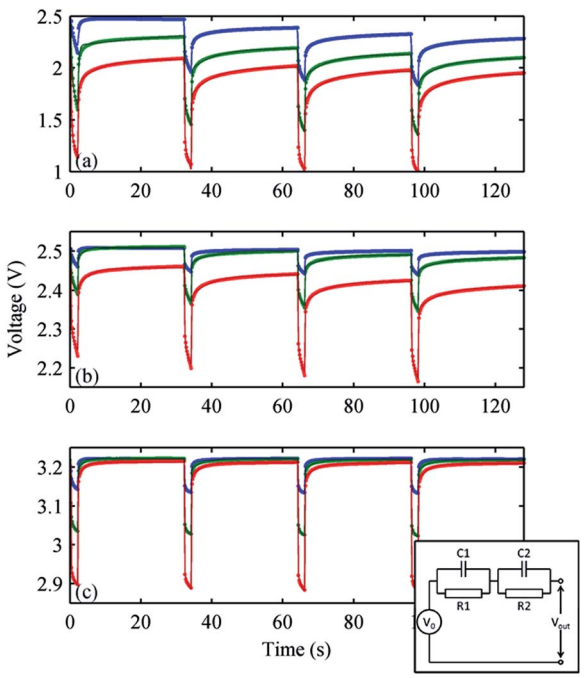

Fig. 4 Galvanostatic discharge/recover results for batteries made using (a) monolayer graphene, (b) graphite paper and (c) graphene foam; 100 μA (blue), 250 μA (green) and 500 μA (red) discharge currents; circles show experimental data points, solid lines show model fits. Inset: schematic of the equivalent circuit model.

To fit the model parameters V_0, R_1, R_2, C_1 and C_2, the values of these parameters were assumed to remain constant over a single discharge/recovery cycle, but allowed to change over subsequent cycles. V_0 is the open circuit voltage and R_1, R_2, C_1 and C_2 are series impedance elements in the battery. Trial discharge/recovery cycle curves were calculated by solving the above equations numerically, and an iterative least squares non-linear regression algorithm was used to fit the model to the experimental data (using the MATLAB *nlinfit* function). As shown in Fig. 4, such macroscopic double-polarisation equivalent circuit can well-describe the experimentally observed battery-discharge phenomenon. However, the underlying physics of this dynamic, non-equilibrium system is far from straightforward: the free lithium ions, polymer electrolyte, semiconducting graphene and copper substrate are all interacting elements and cannot be treated independently. Even though we can not assign specific physical meaning to parameters such as C_1 and C_2, macroscopic models that represent complicated underlying physical processes in simple terms are incredibly useful to create meaningful comparisons.

The model fit to the second, third and fourth discharge/recovery cycles was excellent (the initial cycle fit was typically of much worse quality) – average model parameters extracted from the fitting are shown in ESI Table S1.† The values of capacitance *etc.* discussed in the following are corresponding to these discharge/charge cycles. While the model has been derived heuristically, we note that the relatively large capacitance values (as large as $\sim$5 mF cm^{-2} for graphene foam) are correlated with the formation of Helmholtz double-layers at the electrode/electrolyte interface.[18] Interestingly, in both the monolayer graphene battery and the graphene foam battery there is a strong dependence of C_1 on discharge current, suggesting that the distance between the Helmholtz planes, the permittivity of the intervening electrolyte or the electrochemical properties of the electrodes are changing with current flow; however, this effect is not seen in the graphite paper battery, and so is likely related to the fact that Li^+ ion intercalation is suppressed at the graphene interface. It was recently reported that a monolayer graphene electrode has a very different specific surface area and area-normalized capacitance[19] than a graphite electrode. A smaller area-normalized capacitance for conventional graphite electrodes was explained by invoking a space charge capacitance, representing a spread of induced electrode charge into the bulk, in series with the Helmholtz capacitance located on the electrolyte side of interface, between the electrolyte and bulk solid. The enhanced capacitance for mono- and few-layer graphene electrodes was attributed to correlations between the π-band electron Fermi liquid and ions in the Helmholtz layer (quantum capacitance).[20] This voltage-correlated quantum capacitance[18] may be related to the dependence of C_1 on discharge current for graphene-based electrodes; however a full understanding of how these are related requires a self-consistent thermoelectric model of the interactions between graphene, copper, lithium ions and electrolyte, which is beyond the scope of this paper.

The recovery effect behaviour seen in Fig. 3 could potentially be caused by non-zero leakage currents recharging the battery when the test equipment was set to zero load current. To confirm that this was not the case, similar discharge/recovery cycles were performed using a metal-film resistor to load the batteries, connected to the battery *via* a relay switch, and with the voltage monitored using a Keithley 6517A electrometer with sub-femtoamp leakage currents. The results (ESI Fig. S3†) show equivalent behaviour to the galvanostatic measurements; furthermore, the behaviour was seen to persist over several hours and many hundreds of cycles.

Conclusions

We have fabricated standard coin cell batteries which differ solely in the nanoarchitecture of the carbon used to construct the battery electrode. However we find that the electrochemical properties of these batteries are strongly determined by that carbon nanoarchitecture: CV measurements confirmed that Li^+ ion intercalation is not a factor in both monolayer graphene and graphene foam electrodes, and discharge measurements demonstrated that the capacity of the battery can be greatly increased by using a foam electrode structure. Furthermore, galvanostatic measurements have shown that, while the dynamic discharge and recovery behaviour of the battery is well described by a double RC model in all cases, the parameter values (both in terms of absolute value and dependence on other variables) are dependent on the nanoarchitecture of the battery.

In summary, we have shown that graphene is different than graphite when used in battery electrodes; additionally, the energy capacity and dynamic response can be optimised by changing the graphene architecture. The electrode nanoarchitecture requires careful consideration as a fundamental material property that can strongly influence the electrochemical performance of the battery.

Acknowledgements

The research leading to these results has received funding from the European Union Seventh Framework Programme under grant agreement no. 604391 Graphene Flagship.

Notes and references

1 M. Armand and J.-M. Tarascon, *Nature*, 2008, **451**, 652.
2 J. R. Dahn, T. Zheng, Y. Liu and J. S. Xue, *Science*, 2013, **270**, 590.
3 Z.-S. Wu, W. Ren, L. Xu, F. Li and H.-M. Cheng, *ACS Nano*, 2011, **5**, 5463.
4 Y.-J. Xu, X. Liu, G. Cui, B. Zhu, G. Weinberg, R. Schlogl, J. Maier and D. S. Su, *ChemSusChem*, 2010, **3**, 343.
5 D. Wei, S. Haque, P. Andrew, J. Kivioja, T. Ryhänen, A. Pesquera, A. Centeno, B. Alonso, A. Chuvilin and A. Zurutuza, *J. Mater. Chem. A*, 2013, **1**, 3177.
6 B. Partoens and F. Peeters, *Phys. Rev. B: Condens. Matter Mater. Phys.*, 2006, **74**, 075404.
7 E. S. Reich, *Nature*, 2014, **506**, 19.

8 J. Baringhaus, M. Ruan, F. Edler, A. Tejeda, M. Sicot, A.-P. Li, Z. Jiang, E. H. Conrad, C. Berger, C. Tegenkamp and W. A. de Heer, *Nature*, 2014, **0**, 1.
9 E. Pollak, B. Geng, K.-J. Jeon, I. T. Lucas, T. J. Richardson, F. Wang and R. Kostecki, *Nano Lett.*, 2010, **10**, 3386.
10 E. Lee and K. A. Persson, *Nano Lett.*, 2012, **12**, 4624.
11 B. Z. Jang, C. Liu, D. Neff, Z. Yu, M. C. Wang, W. Xiong and A. Zhamu, *Nano Lett.*, 2011, **11**, 3785.
12 H. Ji, L. Zhang, M. Pettes, H. Li, S. Chen, L. Shi, R. Piner and R. Ruoff, *Nano Lett.*, 2012, **12**, 2446.
13 Y. Kato, K. Hasumi, S. Yokoyama, T. Yabe and H. Ikuta, *Solid State Ionics*, 2002, **150**, 355.
14 L. Gan, D. Zhang and X. Guo, *Small*, 2012, **8**, 1326.
15 C. Wang, A. J. Appleby and F. E. Little, *Electrochim. Acta*, 2001, **46**, 1793.
16 Y.-Y. Hu, Z. Liu, K.-W. Nam, O. J. Borkiewicz, J. Cheng, X. Hua, M. T. Dunstan, X. Yu, K. M. Wiaderek, L.-S. Du, K. W. Chapman, P. J. Chupas, X.-Q. Yang and C. P. Grey, *Nat. Mater.*, 2013, **12**, 1130.
17 H. He, R. Xiong and J. Fan, *Energies*, 2011, **4**, 582.
18 M. D. Stoller, C. W. Magnuson, Y. Zhu, S. Murali, J. W. Suk, R. Piner and R. S. Ruoff, *Energy Environ. Sci.*, 2011, **4**, 4685.
19 H. Ji, X. Zhao, Z. Qiao, J. Jung, Y. Zhu, Y. Lu, L. L. Zhang, A. H. Macdonald and R. S. Ruoff, *Nat. Commun.*, 2014, **5**, 3317.
20 J. Xia, F. Chen, J. Li and N. Tao, *Nat. Nanotechnol.*, 2009, **4**, 505.